magnetochemistry

MDPI

Article

Superconductivity and Fermi Surface Studies of β''-(BEDT-TTF)$_2$[(H$_2$O)(NH$_4$)$_2$Cr(C$_2$O$_4$)$_3$]·18-Crown-6

Brett Laramee [1,†], Raju Ghimire [1,†], David Graf [2], Lee Martin [3], Toby J. Blundell [3] and Charles C. Agosta [1,*]

[1] Department of Physics, Clark University, Worcester, MA 01610, USA
[2] National High Magnetic Field Lab, Tallahassee, FL 32310-3706, USA
[3] School of Science and Technology, Nottingham Trent University, Nottingham NG11 8NS, UK
* Correspondence: cagosta@clarku.edu
† These authors contributed equally to this work.

Abstract: We report rf-penetration depth measurements of the quasi-2D organic superconductor β''-(BEDT-TTF)$_2$[(H$_2$O)(NH$_4$)$_2$Cr(C$_2$O$_4$)$_3$]·18-crown-6, which has the largest separation between consecutive conduction layers of any 2D organic metal with a single packing motif. Using a contactless tunnel diode oscillator measurement technique, we show the zero-field cooling dependence and field sweeps up to 28 T oriented at various angles with respect to the crystal conduction planes. When oriented parallel to the layers, the upper critical field, $H_{c2} = 7.6$ T, which is the calculated paramagnetic limit for this material. No signs of inhomogeneous superconductivity are seen, despite previous predictions. When oriented perpendicular to the layers, Shubnikov–de Haas oscillations are seen as low as 6 T, and from these we calculate Fermi surface parameters such as the superconducting coherence length and Dingle temperature. One remarkable result from our data is the high anisotropy of H_{c2} in the parallel and perpendicular directions, due to an abnormally low $H_{c2\perp} = 0.4$ T. Such high anisotropy is rare in other organics and the origin of the smaller $H_{c2\perp}$ may be a consequence of a lower effective mass.

Keywords: organic conductors; 2D metals; anisotropic superconductivity

Citation: Laramee, B.; Ghimire, R.; Graf, D.; Martin, L.; Blundell, T.J.; Agosta, C.C. Superconductivity and Fermi Surface Studies of β''-(BEDT-TTF)$_2$[(H$_2$O)(NH$_4$)$_2$Cr(C$_2$O$_4$)$_3$]·18-Crown-6. *Magnetochemistry* **2023**, *9*, 64. https://doi.org/10.3390/magnetochemistry9030064

Academic Editors: Laura C. J. Pereira and Dulce Belo

Received: 26 January 2023
Revised: 14 February 2023
Accepted: 20 February 2023
Published: 24 February 2023

1. Introduction

Many crystalline organic conductors are highly anisotropic, consisting of alternating conducting cation layers and quasi-insulating anion layers [1–3]. The organic metal β''-(BEDT-TTF)$_2$[(H$_2$O)(NH$_4$)$_2$Cr(C$_2$O$_4$)$_3$]·18-crown-6 (hereafter β''(ET)Cr, for short) is a quasi-2D (Q2D) superconductor that has an extraordinarily wide anion layer spacing, $s = 27.38$ Å [4], compared to other well-known organics such as κ-(ET)$_2$Cu(NCS)$_2$, where $s = 15$ Å [5]. Anisotropic metals, such as these Q2D crystals, tend to support many correlated electron states such as charge density waves, spin density waves, and superconductivity, because the constrained motion of the carriers enhances the electron–electron interactions. It is therefore useful to study these materials to learn about the origin and stability of correlated electron states. Although they tend to only support these correlated states at low temperatures, <10 K, they are generally electronically clean systems with long mean free paths, allowing the use of quantum oscillations to study the Fermi surface and learn about the detailed band structure, in addition to studying the correlated ground states [6]. Moreover, layered anisotropic superconductors can display a wide variety of anisotropic behaviours when subjected to external magnetic fields oriented at different angles with respect to the conducting planes, including highly anisotropic superconducting critical fields [7], inhomogeneous superconductivity [8], and novel vortex effects [9].

The wide anion layer spacing coupled with a reasonable superconducting critical temperature, T_c, make β''(ET)Cr a prime candidate to support the inhomogeneous superconducting FFLO state. Proposed independently in 1964 and 1965 by Fulde and Ferrell [10] and Larkin and Ovchinnikov [11], the FFLO state is an exotic superconducting state at

high fields and low temperatures where superconductivity survives past the Clogston–Chandrasekhar paramagnetic limit, H_P, where the Zeeman splitting energy would ordinarily overcome the binding energy of the Cooper pairs. In this state, the total momentum of the Cooper pairs is non-zero, and the superconducting order parameter is modulated. As a good approximation, $H_P = \sqrt{2}\Delta_s / g\mu_B$, where Δ_s is the superconducting energy gap, g is the Landé g-factor, and μ_B is the Bohr magneton. For β''(ET)Cr, $\mu_0 H_P = 7.6$ T [4]. In order to reach H_P, however, the orbital destruction of superconductivity needs to be suppressed. For layered organics, magnetic flux lines can penetrate through the quasi-insulating anion layers when the field is aligned parallel to the conduction planes, suppressing the orbital destruction of superconductivity in the cation layers. The wide anion layer of β''(ET)Cr should lead to a large Maki parameter $\alpha_M = \sqrt{2}H^0_{orb}/H_P$, where H^0_{orb} is the orbital critical field in the parallel direction, thus favouring the paramagnetic destruction of Cooper pairs [12]. In this case, the FFLO state is favoured for superconductors in the clean limit.

A contactless tunnel diode oscillator measurement technique is used to measure the penetration depth, λ, of the electromagnetic field into the sample. The penetration depth comes from the addition of two parts, λ_L and λ_v, the London penetration depth and the penetration depth due to motion of the vortices, respectively, following the equation

$$\lambda^2 = \lambda_L^2 + \frac{B\Phi_0}{4\pi k_p}, \quad (1)$$

where B is the magnetic field, Φ_0 is the quantum flux, and k_p is the restoring force on the vortices [13]. In the data, $\Delta f \propto \lambda$, where a lower frequency corresponds to a smaller penetration depth, indicating better superconductivity. Similarly, a lower frequency corresponds to less movement of the vortices or a greater restoring force.

Previous temperature sweeps down to 1 K at constant external magnetic fields showed some signs pointing towards the FFLO state, but no confirmation was given [4]. In this article we show a zero-field cooling curve which confirms the previously reported T_c of roughly 4 K. At a base temperature of 60 mK, we present B-field sweeps both parallel and perpendicular to the conduction layers of the sample. When oriented parallel to the layers, where the magnetic field is in the crystallographic a/b plane, we find no evidence of the FFLO state, contrary to the previous prediction, and the superconductivity does not extend above H_P. When oriented perpendicular to the layers, along the c axis, single frequency Shubnikov–de Haas oscillations are observed up to 28 T. Analysis of the oscillations give the Dingle temperature, T_D [K], and subsequently, the mean free path, l [Å]. The mean free path was calculated to be slightly greater than the superconducting coherence length, but perhaps not enough to stabilize the FFLO state.

The upper critical fields, H_{c2}, of β''(ET)Cr in the $B_\parallel$ and $B_\perp$ orientations are surprisingly anisotropic. With $T_c \approxeq 4$ K, $H_{c2\parallel} = H_P = 7.6$ T is not abnormal, but the observed $H_{c2\perp} = 0.4$ T is unusually low. We compare this anisotropy with other well-known Q2D organics along with other Fermi surface parameters. Further study is needed into the mechanism behind the low perpendicular upper critical field and other potential effects of the high crystal anisotropy on the properties of the material.

2. Materials and Methods

Single crystals of β''-(BEDT-TTF)$_2$[$(H_2O)(NH_4)_2Cr(C_2O_4)_3$]·18-crown-6 were grown by electrocrystallization as described in [4]. The structure of the layering gives this crystal the widest gap between consecutive conducting (ET) layers of any organic superconductor with a single packing motif (β''), making this material of particular interest for studying Q2D systems.

A contactless tunnel diode oscillator (TDO) penetration depth technique was used to measure the change in frequency of a self-resonant circuit containing the crystal inside an inductor [14]. As the crystal expels the rf field, the complex impedance of the inductor in the resonant circuit changes, which is a function of relative rf-penetration depth, $\Delta\lambda$, a sum of the London penetration depth and penetration due to motion of vortices in a Type-II

superconductor, as seen in Equation (1). Therefore, $\Delta f = \Delta f(\lambda)$, where we monitor Δf with a frequency counter or lock-in amplifier. At fields above H_{c2}, the TDO measures the normal-state skin depth, $\Delta\delta$. At cryogenic temperatures, the signal-to-noise ratio of the TDO fundamental frequency results in a resolution of about one part in 10^7, making the TDO technique sensitive to tiny variations in small samples without requiring contacts.

Experiments were performed at the National High Magnetic Field Laboratory (NHMFL) in Tallahassee, FL in a 32 T DC all-superconducting magnet containing a top loading dilution refrigerator. The data presented in this paper comes from two separate single-crystals grown in the same batch, both having a largest in-plane dimension of roughly 750 μm. Each single-crystal was placed inside an 810 μm diameter four-turn coil connected to a TDO circuit board by approximately 2 cm of a twisted wire pair. The coils and TDO circuits were placed on a single-axis rotator probe alongside a calibrated RuO thermometer for temperature measurements. Zero-field cooling conditions were identical for the two crystals as the distance between them was about 1 cm. The fundamental frequencies of the TDOs were 639 and 453 MHz, respectively, which were mixed down to 0.5–10 MHz using a superheterodyne receiver.

After reaching base temperature, the samples were rotated in a finite DC field in order to determine when the orientation of the field was parallel to the conducting layers of the samples. The conducting layers of crystals 1 and 2 were askew by roughly 5.6°. Field-dependent data was collected by rotating to a fixed angle and increasing the field.

3. Results

The zero-field cooling dependence of crystal 2 is shown in Figure 1. The superconducting transition at $T_c = 3.9$ K is broad but comparable to the previous reported value [4], and the transition spans roughly 4 MHz, a sizeable signal strength. Note that the absolute TDO frequency measurement is proportional to relative rf-penetration depth, so the absolute scale for λ is arbitrary. Crystal 1, not shown, has a much less obvious superconducting transition spanning only 0.8 MHz at a lower temperature, suggesting that it was a weaker superconductor than crystal 2. Despite the crystal quality discrepancy, crystal 1 yielded results that supported our findings from crystal 2 throughout the duration of the experiment.

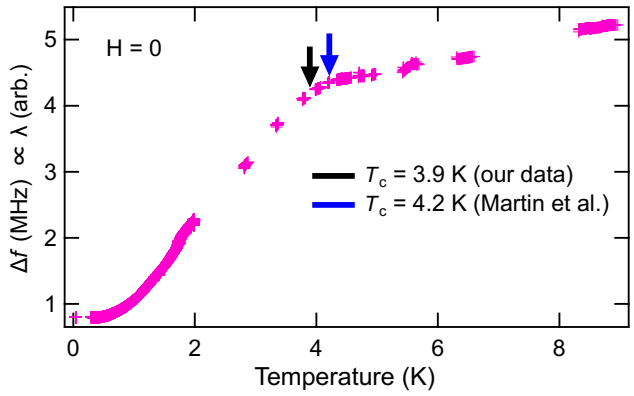

Figure 1. Rf-penetration depth as a function of temperature in a zero magnetic field. The critical temperature, defined by the minimum of $d^2\lambda/dT^2$, is similar to previous work [4].

After reaching a base temperature of 60 mK, a series of field sweeps at different angles tracked $H_{c2}(\theta)$. A subset of these field sweeps is shown in Figure 2a between $\theta = -14°$ and +2°. Near $B_{\|}$ ($\theta = 0°$), the superconducting transition is broad, with the highest H_{c2} recorded to be 7.6 T at $\theta = \pm 0.25°$ (green). Away from $B_{\|}$, the superconducting transition becomes sharper and decreases in field. Despite the wide anion layer being a promising indicator that the crystal might be able to harbour the FFLO state, no evidence was found from our field sweep data. The field sweeps nearest to $\theta = 0°$ showed superconductivity persisting only up to $H_P = 7.6$ T, and no anomalous bumps in the 2nd derivatives indicating a transition to the FFLO state were found.

Though the anion layer spacing in β''(ET)Cr is wide compared to other organics, the cryogenic temperatures at which the experiment was performed should be well below any dimensional crossover transition. Therefore, $H_{c2}(\theta)$ in Figure 2b follows the Tinkham thin-film formula for a 2D layered Josephson-coupled superconductor,

$$\left|\frac{H_{c2}(\theta)\cos(\theta)}{H_{c2\perp}}\right| + \left[\frac{H_{c2}(\theta)\sin(\theta)}{H_{c2\parallel}}\right]^2 = 1 \quad (2)$$

as opposed to anisotropic Ginzburg–Landau theory [7,15]. Though Equation (2) is based on the orbital destruction of superconductivity only, it gives reasonable agreement to the data. One remarkable result is the high anisotropy in the ultimate critical fields in the parallel vs. perpendicular orientations, with $H_{c2\parallel}/H_{c2\perp} = 19$, coming from a low $H_{c2\perp}$.

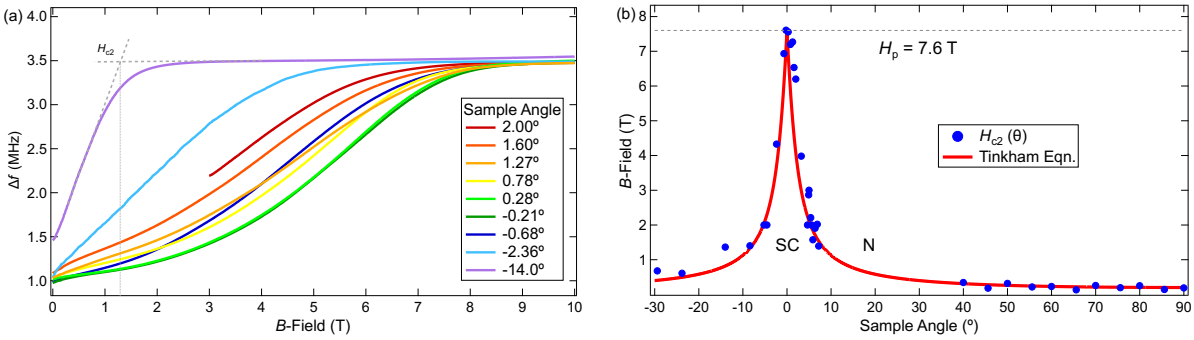

Figure 2. (**a**) Rf-penetration depth as a function of the magnetic field oriented at different angles with respect to the conducting planes of the sample, with $B_{\parallel} = 0°$. Field sweeps were performed at $T < 100$ mK. We define H_{c2} as the crossing point of the linear extrapolations above and below the superconducting transition, shown in grey. (**b**) $H_{c2}(\theta)$ as taken from (**a**) and from additional data not shown. The solid trace is the 2D Tinkham thin-film equation, Equation (2).

Due to trapped flux in the 32 T superconducting magnet, the given magnetic field, which is reported based on the current in the magnet, may be lower than the real field experienced by the crystals. Therefore, $H_{c2\perp} = 0.2$ T seen in the raw data is a lower bound. We estimate the range of the magnitude of trapped flux could be 0.15–0.25 T at low fields, based on discussion with the NHMFL. Therefore, $H_{c2\perp}$ = 0.2 + (0.15 − 0.25) T, with the most likely value for $H_{c2\perp}$ = 0.4 T. Later, we show orbital critical field calculations that are close to this corrected value.

Field sweeps with the magnetic field oriented far from parallel to the conduction layers of the crystal are shown in Figure 3. At $\theta_{\perp} = 90°$, strong, pure sinusoidal oscillations are seen. At $\theta \approxeq 60°$ the amplitude of the SdH oscillations pass through zero and the phase flips, indicating a spin-zero. This occurs when the Landau level spacing $\Delta E_L = \hbar eB/m^*$ is an integer multiple of the Zeeman splitting energy $\Delta E_Z = g\mu_B B$, where the effective mass $m^*(\theta) = m^*_{\perp}/\sin(\theta)$ in our convention. By fitting the SdH oscillation amplitudes as a function of the angle to the Lifshitz–Kosevich (L–K) formula [16], we determine $g^* = 1.89$. According to McKenzie [17], this value of g is lower than expected due to the highly correlated nature of the quasi-particles in these lower-dimensional materials, not unlike how the effective mass m^* is different from the band mass as calculated from the band structure. Therefore, the g-factor as measured by electron spin resonance, which we will refer to as g, is probably still very close to two. The measured g-factor from the location of the spin-zero, g^*, will be enhanced or diminished by many body effects. In this case, $g^* = 1.89$, and the ratio $g^*/g = 0.95$, a value comparable to other organic conductors, as seen in McKenzie's paper [17].

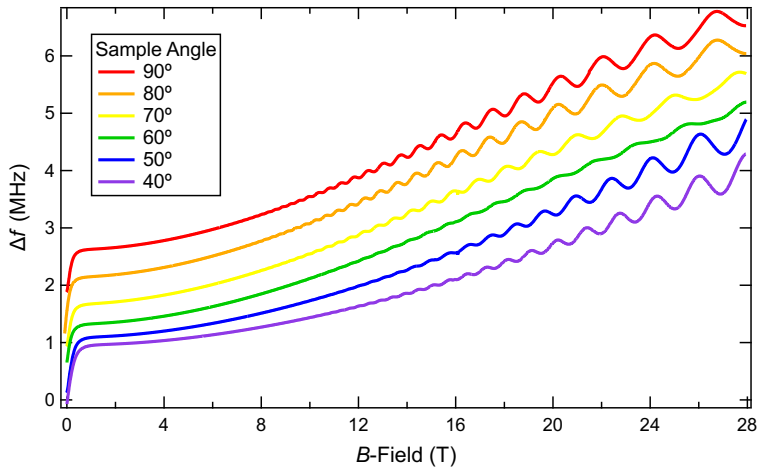

Figure 3. Field sweeps up to 28 T at different angles with respect to the layers of the sample. At $B_\perp = 90°$, quantum oscillations begin as low as 6 T. The data are offset vertically for clarity.

As shown in Figure 4, Shubnikov–de Haas oscillations can be seen as low as 6 T (a) and are of a single frequency of $\alpha = 253$ T (b). There is no evidence of breakdown orbits, and the next highest peak is the 2nd harmonic, which is almost four orders of magnitude weaker than the fundamental. $F_{\mathrm{SdH}}(\theta)$ follows the expected behaviour for a 2D metal with a corresponding cylindrical Fermi surface (c). From the SdH oscillation amplitudes we construct the Dingle plot shown in (d). The Dingle temperature is a measure of the scattering (purity) in a crystal; $T_{\mathrm{D}} = X/14.7m^*(\theta)$, where X is the slope of the log of the oscillation amplitudes vs. B^{-1}. Using the previously reported $m^*_\perp = 1.4m_e$ [4], we find $T_{\mathrm{D}} = 2.42$ K for crystal 2 and $T_{\mathrm{D}} > 4$ K for crystal 1, confirming that crystal 2 is a cleaner superconductor.

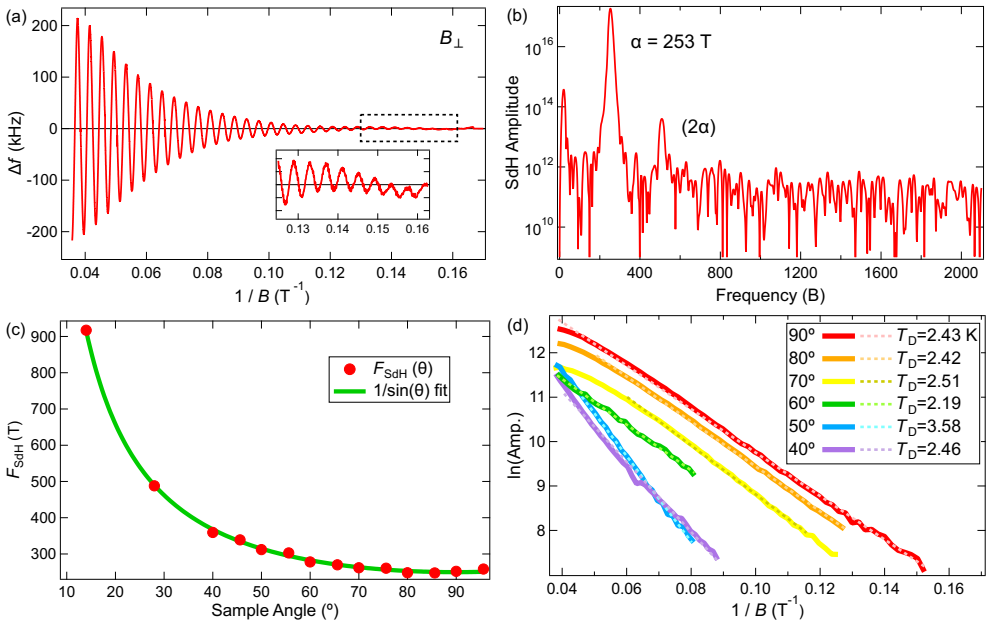

Figure 4. (**a**) Shubnikov–de Haas oscillations ($\theta = 90°$ from Figure 3) with the background subtracted and plotted against $1/B$. Inset: zoom of main figure; oscillations can be seen down to 6 T. (**b**) FFT of (**a**). A singular α frequency can be observed, as well as its weaker 2nd harmonic. (**c**) $F_{\mathrm{SdH}}(\theta)$ as gathered by field sweeps at different angles. The data follows the expected $1/\cos(\theta)$ dependence for a cylindrical Fermi surface, noting that our convention of $B_\perp = 90°$ is reverse to the traditional $B_\perp = 0°$. (**d**) Dingle plot produced by the data shown in Figure 3, reduced as in (**a**). Linear fits are overlaid on the data with corresponding Dingle temperatures.

4. Discussion

The temperature sweep data in Figure 1 yields a similar $T_c \approxeq 4$ K to previous work [4]. We previously found that cooling rate could affect whether or not the crystal exhibits superconductivity, perhaps due to a structural transition at higher temperatures. Because two of our crystals underwent identical experimental cooling, however, the variation in their properties due to cooling rate may not be the only factor that determines the quality of samples. It is now clearer that there may be intrinsic disorder in the samples that also determines the strength of the superconductivity, and crystal variation could be a challenge in future experiments.

Field sweeps up to 28 T were performed below 100 mK, extending the reach of previous work in both field and temperature. Previous results down to 1 K [4] suggested the possibility of forming the FFLO state at low temperatures and high magnetic fields above H_P. Despite this, the λ(B) data close to $B_{\parallel}$, Figure 2, show H_{c2} as not surpassing the Clogston–Chandrasekhar paramagnetic limit and no FFLO state is observed. The 2D Tinkham thin-film equation produces an agreeable fit to our $H_{c2}(\theta)$ plot.

The anisotropy of $H_{c2\parallel}/H_{c2\perp}$ is noteworthy being higher than most other well-known 2D organic superconductors, and a comparison with other similar superconductors in Table 1 shows that the low $H_{c2\perp}$ is anomalous. Using the corrected value of 0.4 T for $H_{c2\perp}$, $H_{c2\parallel}/H_{c2\perp} \approxeq 19$, which is only less than κ-$(ET)_2I_3$ in terms of anisotropy magnitude, and higher than the others.

Table 1. A comparison of crystal properties from experimental results to other well-known quasi-2D organic superconductors. The title compound and its corresponding values are shown in bold.

Crystal Name [Citations]	T_c (K)	$H_{c2\parallel}$ (T)	$H_{c2\perp}$ (T)	H^0_{orb} (T)	H_P (T)	m^*/m_e	l (Å)	$\xi_{\parallel}$ (Å)
κ-$(ET)_2Cu(NCS)_2$ [18–20]	9.6	28	6	17.6 †	21.6	3.5	900	74
β''-$(ET)_2SF_5CH_2CF_2SO_3$ [6,21,22]	4.5	11	1.6	2.07 †	9.2	2.0	520	122
λ-$(BETS)_2GaCl_4$ [23–25]	4.3	11	2.9	1.6 †	8.3	3.6	170	107
β''(ET)Cr [4]	**4.1**	**7.6**	**0.4**	**0.49**	**7.6**	**1.4**	**367**	**286**
κ-$(ET)_2I_3$ [26–28]	3.5	6.7	0.2	1.37	5.7	3.9	953	410
α-$(ET)_2NH_4Hg(SCN)_4$ [7,29,30]	0.96	2.1	0.12	0.05 †	2.1	2.5	663	605

† H^0_{orb} with daggers use Equation (5) with Δ_s from specific heat data. Others use Equation (4), the BCS result.

Away from $B_{\parallel}$, we show Shubnikov–de Haas oscillations, Figure 3, at multiple field angles with respect to the conduction layers of the crystal. Up to 28 T and as low as 6 T, we find strong, harmonically pure oscillations. At $B_{\perp}$, the fundamental frequency is 253 T, slightly higher than the previously reported $F_{SdH} = 231.1$ T [4]. The oscillation frequencies follow the expected $1/\sin(\theta)$ behaviour as we rotate the sample (often reported as $1/\cos(\theta)$ when $B_{\perp} = 0°$). We report the Dingle temperature $T_D = 2.4$ K in our main crystal and $T_D > 4$ K in the other, noisier crystal.

Using the Shubnikov–de Haas oscillations and the effective mass, we can calculate the Fermi surface parameters such as the Fermi velocity, $v_F = \sqrt{2\hbar e F_{SdH}}/m^*$, the scattering time, which is related to the Dingle temperature, $\tau = \hbar/2\pi k_B T_D$, and the mean free path $l = v_F\tau$. For the superconducting coherence length, ξ, we use Equation (3), with $H_{c2\perp} = 0.4$ T at $T < 100$ mK. These parameters are shown in Table 1 alongside comparisons to other Q2D organic superconductors. One of the conditions for forming the FFLO state is for the crystal to be in the clean limit, i.e., $r = l/\xi > 1$, which is barely satisfied for β''(ET)Cr, though this alone is no guarantee of FFLO stabilization, as seen in the paramagnetically limited α-$(ET)_2NH_4Hg(SCN)_4$ [7].

Considering that the remarkably low $H_{c2\perp}$ is well below H_P, we would expect the orbital effect to dominate the destruction of superconductivity, following the equation

$$H_{c2\perp} \approxeq H^0_{orb} = \frac{\Phi}{2\pi\xi^2_{\parallel}}, \quad (3)$$

where $\xi = \hbar v_F / \pi \Delta_s$, v_F is the Fermi velocity, and the superconducting energy gap is given by the BCS result, $\Delta_s = 1.75 k_B T_c$, resulting in

$$H^0_{orb} = \frac{\Phi}{2\pi} \left(\frac{1.75 \pi k_B T_c}{\hbar v_F} \right)^2. \quad (4)$$

With v_F as calculated above, $T_c = 3.9$ K, and using the BCS result, we arrive at $H^0_{orb} = 0.49$ T, very close to our measured $H_{c2\perp}$. We note that, once specific heat data are taken, the equation for H^0_{orb} could be made more accurate using Δ_s calculated empirically via the Alpha model [20,31,32] rather than the BCS result, using the equation

$$H^0_{orb} = \frac{\Phi \pi \Delta_s^2 m^*}{4\hbar^2 E_F}, \quad (5)$$

where $E_F = \hbar e F_{SdH}$ is the Fermi energy.

Orbital critical field calculations do agree moderately well with $H_{c2\perp}$ for most of the organics in Table 1, with the exceptions of κ-$(ET)_2Cu(NCS)_2$ and κ-$(ET)_2I_3$. The former can be justified by taking into account Zeeman pair breaking and strong coupling. The calculated H^0_{orb} for κ-$(ET)_2Cu(NCS)_2$ is close to the value of H_P, where one would expect a large contribution of Zeeman pair breaking to limit the upper critical field, as calculated by the the WHH formula [33], and is seen as a downward curvature in $H_{c2\perp}$(T) [2]. The rest of the materials in Table 1 have relatively linear $H_{c2\perp}$(T) phase diagrams, given that H^0_{orb} is much less than H_P for all of them. However, new measurements may be needed to account for the discrepancy between $H_{c2\perp}$ and the calculated H^0_{orb} for λ-$(BETS)_2GaCl_4$ and α-$(ET)_2NH_4Hg(SCN)_4$, as one would not expect H^0_{orb} to be less than the measured critical field. Finally, the extremely low $H_{c2\perp}$ for κ-$(ET)_2I_3$ cannot be accounted for by measurement error, and another mechanism may be at play in that material.

In fact, many layered organics have $H_{c2\perp}$(T) phase diagrams that do not follow the simple model suggested by Equation (3) or even more complicated models such as the WHH formula. Although there have been some attempts to build separate theories for H_{c2}(T) in layered superconductors, they have tended to focus on the parallel orientation with the magnetic field along the layers [15,34] or address special cases such as the diverging perpendicular critical fields of some cuprates or dichalcogenides, motivating proposed mechanisms based on magnetic impurities [35] or quantum critical behaviour [36], neither of which are suggested for organic materials. There are possible instances of 3D-to-2D crossover in the perpendicular critical fields of layered organic superconductors [25,37], but there is no theory that supports 3D-to-2D crossover in perpendicular magnetic fields.

5. Conclusions

In this brief report we present high-field, low-temperature measurements on β''(ET)Cr, a layered crystalline organic superconductor with novel crystal geometry, using a tunnel diode oscillator measurement technique. Despite prior predictions, inhomogeneous superconductivity was not found, and the superconductor may be paramagnetically limited. From a series of strong Shubnikov–de Haas oscillations, we calculated Fermi surface parameters confirming the crystal to be in the clean limit, though only just. We found that this material exhibits higher critical field anisotropy than other well-known organics, with H_{c2} in the perpendicular-to-the-layers orientation being surprisingly low. Though, calculation of the expected orbital critical field matches the measured value. This raises further questions as to why other organics do not necessarily follow this behaviour.

Future additional field sweep experiments would help clarify multiple points regarding the properties of β''(ET)Cr presented in this work. In the $B_\perp$ direction, collecting SdH oscillation data at multiple temperatures is of utmost importance to confirm the effective mass value, $m^* = 1.4$ K, reported by Martin et al. [4], which is used in numerous calculations of Fermi surface parameters, the orbital critical field, Equation (5), etc.

In particular, the estimated g-factor, $g^* = 1.89$, could be made more accurate both by confirming m^* and by gathering additional SdH amplitude data at finer angle intervals. Fitting the oscillation amplitudes to the L–K formula produced error bars that were significant, due to limited angular sample size, and only one spin-zero was seen. As an alternative to field sweeps at fixed angles, since $\alpha = 253$ T is the only visible SdH frequency, rotating the sample in a high DC field would immediately reveal at what spin-zero angles the oscillations vanished, which uniquely determine the product m^*g^* [17,38].

The H/T phase diagrams of the upper critical fields in both the $B_{\parallel}$ and $B_{\perp}$ orientations would benefit from being completed, as this present work only adds data at $T = 60$ mK, a temperature well below the previously published data [4], leaving a gap in the $0.1 < T < 1$ K range. A saturation of $H_{c2\parallel}$(T) to a constant value in this region would help confirm whether the crystal is paramagnetically limited [7] and determine the degree to which many-body effects might enhance H_P [17]. The suspected linearity of $H_{c2\perp}$(T) in this temperature range should also be investigated, as discussed above, to deepen our understanding of perpendicular critical field phase diagrams in layered organics, where the extent of the current theory is incomplete.

Author Contributions: Conceptualization, C.C.A. and L.M.; formal analysis, B.L.; investigation, B.L., R.G. and D.G.; writing, B.L. and C.C.A.; sample synthesis, T.J.B. and L.M.; funding acquisition, C.C.A. All authors have read and agreed to the published version of the manuscript.

Funding: This research was funded by the NSF Agreement No. DMR-1905950. L.M. and T.J.B. thank the Leverhulme Trust for funding for synthesis of crystals (LT170022). A portion of this work was performed at the National High Magnetic Field Laboratory, which is supported by National Science Foundation Cooperative Agreement No. DMR-1644779 and the State of Florida.

Institutional Review Board Statement: Not Applicable.

Informed Consent Statement: Not Applicable.

Data Availability Statement: The data presented in this study are available on request from the corresponding author.

Conflicts of Interest: The authors declare no conflict of interest.

References

1. Ishiguro, T.; Yamaji, K.; Saito, G. *Organic Superconductors*; Springer Series in Solid-State Sciences; Springer: Berlin/Heidelberg, Germany, 1998.
2. Singleton, J.; Mielke, C. Quasi-two-dimensional organic superconductors: A review. *Contemp. Phys.* **2002**, *43*, 63–96. [CrossRef]
3. Lebed, A. *The physics of Organic Superconductors and Conductors*; Springer Series in Materials Sciences; Springer: Berlin/Heidelberg, Germany, 2008; Volume 110.
4. Martin, L.; Lopez, J.R.; Akutsu, H.; Nakazawa, Y.; Imajo, S. Bulk Kosterlitz–Thouless Type Molecular Superconductor β''-(BEDT-TTF)$_2$[$(H_2O)(NH_4)_2Cr(C_2O_4)_3$]·18-crown-6. *Inorg. Chem.* **2017**, *56*, 14045–14052. [CrossRef] [PubMed]
5. Urayama, H.; Yamochi, H.; Saito, G.; Nozawa, K. A new ambient pressure organic superconductor based on BEDT-TTF with T_c higher than 10 K (T_c= 10.4 K). *Chem. Lett.* **1988**, *17*, 55–58. [CrossRef]
6. Wosnitza, J.; Wanka, S.; Hagel, J.; Häussler, R.; Löhneysen, H.V.; Schlueter, J.A.; Geiser, U.; Nixon, P.G.; Winter, R.W.; Gard, G.L. Shubnikov—De Haas effect in the superconducting state of an organic superconductor. *Phys. Rev. B* **2000**, *62*, R11973–R11976. [CrossRef]
7. Coffey, T.; Martin, C.; Agosta, C.C.; Kinoshota, T.; Tokumoto, M. Bulk two-dimensional Pauli-limited superconductor. *Phys. Rev. B* **2010**, *82*, 212502. [CrossRef]
8. Agosta, C.C. Inhomogeneous Superconductivity in Organic and Related Superconductors. *Crystals* **2018**, *8*, 285. [CrossRef]
9. Mansky, P.; Danner, G.; Chaikin, P. Vortex pinning and lock-in effect in a layered superconductor with large in-plane anisotropy. *Phys. Rev. B (Condens. Matter)* **1995**, *52*, 7554–7563. [CrossRef] [PubMed]
10. Fulde, P.; Ferrell, R.A. Superconductivity in a Strong Spin-Exchange Field. *Phys. Rev.* **1964**, *135*, A550–A563. [CrossRef]
11. Larkin, A.I.; Ovchinnikov, Y.N. Inhomogeneous State of Superconductors. *Sov. Phys. JETP* **1965**, *20*, 762.
12. Maki, K. Effect of Pauli Paramagnetism on Magnetic Properties of High-Field Superconductors. *Phys. Rev.* **1966**, *148*, 362–369. [CrossRef]
13. Mansky, P.A.; Chaikin, P.M.; Haddon, R.C. Evidence for Josephson vortices in κ-(BEDT-TTF)$_2$Cu(NCS)$_2$. *Phys. Rev. B* **1994**, *50*, 15929–15944. [CrossRef]

14. Van Degrift, C.T. Tunnel diode oscillator for 0.001 ppm measurements at low temperatures. *Rev. Sci. Instrum.* **1975**, *46*, 599. [CrossRef]
15. Schneider, T.; Schmidt, A. Dimensional crossover in the upper critical field of layered superconductors. *Phys. Rev. B* **1993**, *47*, 5915–5921. [CrossRef] [PubMed]
16. Shoenberg, D. *Magnetic Oscillations in Metals*; Cambridge University Press: Cambridge, UK, 1984.
17. McKenzie, R.H. Wilson's ratio and the spin splitting of magnetic oscillations in quasi-two-dimensional metals. *arXiv* **1999**, arXiv.9905044.
18. Taylor, O.J.; Carrington, A.; Schlueter, J.A. Specific-Heat Measurements of the Gap Structure of the Organic Superconductors κ-(BEDT-TTF)$_2$-Cu[N(CN)$_2$]Br and κ-(ET)$_2$Cu(NCS)$_2$. *Phys. Rev. Lett.* **2007**, *99*, 057001. [CrossRef]
19. Mihut, I.; Agosta, C.; Martin, C.; Mielke, C.; Coffey, T. Incoherent Bragg reflection and Fermi-surface hot spots in a quasi-two-dimensional metal. *Phys. Rev. B* **2006**, *73*, 125118. [CrossRef]
20. Müller, J.; Lang, M.; Helfrich, R.; Steglich, F.; Sasaki, T. High-resolution ac-calorimetry studies of the quasi-two-dimensional organic superconductor κ-(BEDT-TTF)$_2$Cu(NCS)$_2$. *Phys. Rev. B* **2002**, *65*, 140509.
21. Zuo, F.; Su, X.; Zhang, P.; Brooks, J.S.; Wosnitza, J.; Schlueter, J.A.; Williams, J.M.; Nixon, P.G.; Winter, R.W.; Gard, G.L. Anomalous low-temperature and high-field magnetoresistance in the organic superconductor β''-(BEDT-TTF)$_2$SF$_5$CH$_2$CF$_2$SO$_3$. *Phys. Rev. B* **1999**, *60*, 6296–6299. [CrossRef]
22. Sugiura, S.; Terashima, T.; Uji, S.; Yasuzuka, S.; Schlueter, J.A. Josephson vortex dynamics and Fulde-Ferrell-Larkin-Ovchinnikov superconductivity in the layered organic superconductor β''-(BEDT-TTF)$_2$SF$_5$CH$_2$CF$_2$SO$_3$. *Phys. Rev. B* **2019**, *100*, 014515. [CrossRef]
23. Coniglio, W.A.; Winter, L.E.; Cho, K.; Agosta, C.C.; Fravel, B.; Montgomery, L.K. Superconducting phase diagram and FFLO signature in λ-(BETS)$_2$GaCl$_4$ from rf penetration depth measurements. *Phys. Rev. B* **2011**, *83*, 224507. [CrossRef]
24. Tanatar, M.A.; Ishiguro, T.; Tanaka, H.; Kobayashi, H. Magnetic field-temperature phase diagram of the quasi-two-dimensional organic superconductor λ-(BETS)$_2$GaCl$_4$ studied via thermal conductivity. *Phys. Rev. B* **2002**, *66*, 134503. [CrossRef]
25. Mielke, C.; Singleton, J.; Nam, M.S.; Harrison, N.; Agosta, C.C.; Fravel, B.; Montgomery, L.K. Superconducting properties and Fermi-surface topology of the quasi-two-dimensional organic superconductor λ-(BETS)$_2$GaCl$_4$ (BETS=; bis(ethylenedithio)tetraselenafulvalene). *J. Phys. Condens. Matter* **2001**, *13*, 8325–8345. [CrossRef]
26. Wanka, S.; Beckmann, D.; Wosnitza, J.; Balthes, E.; Schweitzer, D.; Strunz, W.; Keller, H.J. Critical fields and mixed-state properties of the layered organic superconductor κ-(BEDT-TTF)$_2$I$_3$. *Phys. Rev. B* **1996**, *53*, 9301–9309. [CrossRef] [PubMed]
27. Wosnitza, J.; Liu, X.; Schweitzer, D.; Keller, H.J. Specific heat of the organic superconductor κ-(BEDT-TTF)$_2$I$_3$. *Phys. Rev. B* **1994**, *50*, 12747–12751. [CrossRef] [PubMed]
28. Harrison, N.; Mielke, C.H.; Rickel, D.G.; Wosnitza, J.; Qualls, J.S.; Brooks, J.S.; Balthes, E.; Schweitzer, D.; Heinen, I.; Strunz, W. Quasi-two-dimensional spin-split Fermi-liquid behavior of κ-(BEDT-TTF)$_2$I$_3$ in strong magnetic fields. *Phys. Rev. B* **1998**, *58*, 10248–10255. [CrossRef]
29. Wang, H.; Carlson, K.; Geiser, U.; Kwok, W.; Vashon, M.; Thompson, J.; Larsen, N.; McCabe, G.; Hulscher, R.; Williams, J. A New Ambient Pressure Organic Superconductor: (BEDT-TTF)$_2$(NH$_4$)Hg(SCN)$_4$. *Physica C* **1990**, *166*, 57–61. [CrossRef]
30. Brooks, J.S.; Chen, X.; Klepper, S.J.; Valfells, S.; Athas, G.J.; Tanaka, Y.; Kinoshita, T.; Kinoshita, N.; Tokumoto, M.; Anzai, H.; et al. Pressure effects on the electronic structure and low-temperature states in the α-(BEDT-TTF)$_2$MHg(SCN)$_4$ organic-conductor family (M=K, Rb, Tl, NH$_4$). *Phys. Rev. B* **1995**, *52*, 14457–14478. [CrossRef]
31. Padamsee, H.; Neighbor, J.; Shiffman, C. Quasiparticle phenomenology for thermodynamics of strong-coupling superconductors. *J. Low Temp. Phys.* **1973**, *12*, 387–411. [CrossRef]
32. Johnston, D.C. Elaboration of the α-model derived from the BCS theory of superconductivity. *Supercond. Sci. Technol.* **2013**, *26*, 115011. [CrossRef]
33. Werthamer, N.R.; Helfand, E.; Hohenberg, P.C. Temperature and Purity Dependence of the Superconducting Critical Field, H_{c2}. III. Electron Spin and Spin-Orbit Effects. *Phys. Rev.* **1966**, *147*, 295–302. [CrossRef]
34. Klemm, R.A.; Luther, A.; Beasley, M.R. Theory of the upper critical field in layered superconductors. *Phys. Rev. B* **1975**, *12*, 877–891. [CrossRef]
35. Kotliar, G.; Varma, C.M. Low-Temperature Upper-Critical-Field Anomalies in Clean Superconductors. *Phys. Rev. Lett.* **1996**, *77*, 2296–2299. [CrossRef] [PubMed]
36. Ovchinnikov, Y.N.; Kresin, V.Z. Critical magnetic field in layered superconductors. *Phys. Rev. B* **1995**, *52*, 3075–3078. [CrossRef] [PubMed]
37. Agosta, C.; Ivanov, S.; Bayindir, Z.; Coffey, T.; Kushch, N.; Yagubskii, E.; Burgin, T.; Montgomery, L. The anomalous superconducting phase diagram of (BEDO-TTF)$_2$ReO$_4$·H$_2$O. *Synth. Met.* **1999**, *103*, 1795–1796. [CrossRef]
38. Wosnitza, J.; Crabtree, G.W.; Wang, H.H.; Geiser, U.; Williams, J.M.; Carlson, K.D. de Haas–van Alphen studies of the organic superconductors α-(ET)$_2$(NH$_4$)Hg(SCN)$_4$ and κ-(ET)$_2$Cu(NCS)$_2$ [with ET = bis(ethelenedithio)-tetrathiafulvalene]. *Phys. Rev. B* **1992**, *45*, 3018–3025. [CrossRef] [PubMed]